Myoelectric or Force control? A comparative study on a soft arm exosuit

Nicola Lotti[1*], Michele Xiloyannis[2], Francesco Missiroli[1], Casimir Bokranz[1], Domenico Chiaradia[3], Antonio Frisoli[3], Robert Riener[2] and Lorenzo Masia[1]

***Abstract*—The intention-detection strategy used to drive an exosuit is fundamental to evaluate the effectiveness and acceptability of the device. Yet, current literature on wearable soft robotics lacks evidence on the comparative performance of different control approaches for online intention-detection. In the present work, we compare two different and complementary controllers on a wearable robotic suit, previously formulated and tested by our group: a model-based myoelectric control (*myoprocessor*), which estimates the joint torque from the activation of target muscles, and a force control that estimates human torques using an inverse dynamics model (*dynamic arm*). We test them on a cohort of healthy participants performing tasks replicating functional activities of daily living involving a wide range of dynamic movements. Our results suggest that both controllers are robust and effective in detecting human-motor interaction, and show comparable performance for augmenting muscular activity. In particular, the biceps brachii activity was reduced by up to 74% under the assistance of the *dynamic arm* and up to 47% under the *myoprocessor*, compared to a no-suit condition. However, the *myoprocessor* outperformed the *dynamic arm* in promptness and assistance during movements that involve high dynamics: the exosuit work normalized with respect to the overall work was $68.84 \pm 3.81\%$ when it was ran by the *myoprocessor*, compared to $45.29 \pm 7.71\%$ during the *dynamic arm* condition. The reliability and accuracy of motor intention detection strategies in wearable device is paramount for both the efficacy and acceptability of this technology. In the present paper, we offer a detailed analysis of the two most widely used control approaches, trying to highlight their intrinsic structural differences and to discuss their different and complementary performance.**

***Index Terms*—Human-machine interfaces; Wearable Robots; Modeling, Control and Learning for Soft Robots; Control Architectures and Programming**

1: Load cell
2: IMUs sensors
3: Load cell amplifier
4: Actuation stage
5: Embedded controller and motor drive stage
6: Controller battery pack
7: Motor drive battery pack

Fig. 1. *Untethered elbow exosuit*. The device used in this study was designed to assist elbow flexion. The exosuit consisted of a wearable orthosis and a back protector, housing a motor, batteries, sensors and electronics. A force sensor (1) and two IMU (2) sensors were used to measure the interaction force and the arm kinematics, respectively. The back protector housed the force sensor amplifier (3), the actuation stage (4), the embedded controller and motor driver (5) and two battery packs (6,7).

I. Introduction

The first-ever engineered exoskeleton was developed with the idea of *"...combining man and machine into an intimate symbiotic unit that will perform as one wedded system."* [1]. In their work, Mosher and colleagues explicitly acknowledged the unparalleled performance of the nervous system in continuously integrating sensory information and processing it to make informed decisions about future actions. Complementing human cognition with machine mechanical power would have resulted in a mighty entity. Notwithstanding their visionary prospective, the effort to match human biomechanics complexity with machine ruggedness had been underestimated, and is still one of the greatest challenges in wearable robotics [2].

Pons nicely pointed out that the human-robot interface (HRI) consists of processes of two different natures [3]: (1) the physical interaction between the device and its user (pHRI) and (2) the exchange of cognitive information between the human and the robot (cHRI).

The recent introduction in robotics of soft materials and exosuits to transfer forces to the human body has allowed a significant improvement of the pHRI [4], solving issues limiting rigid exoskeletons efficacy such as joint misalignment [5] and addition of substantial inertia to the human limbs. Exosuits have been used to achieve unprecedented levels of walking and running economy [6] and accessible assistance to people with neuromuscular disorders [7].

The cHRI has a higher level of complexity, involving the bidirectional communication between user's mind and machine, achievable only by a reliable human-intention detection, and from robot to human, typically achieved via visual, auditory or haptic feedback. Different modalities of detecting user's intention specifically influence the controller robustness and the assistance efficacy.

In absence of invasive interfaces that record signals from

[1]Nicola Lotti, Francesco Missiroli, Casimir Bokranz and Lorenzo Masia are with the Institut für Technische Informatik (ZITI), Heidelberg University, 69120 Heidelberg, Deutschland.

[2]Michele Xiloyannis and Robert Riener are with the Institute of Robotics and Intelligent Systems, ETH Zürich, Zürich, 8092, Switzerland.

[3]Domenico Chiaradia and Antonio Frisoli are with the TeCIP Institute, PERCRO Laboratory, Scuola Superiore Sant'Anna, Pisa 56127, Italy.

* corresponding author: nicola.lotti@ziti.uni-heidelberg.de

neural implants, the widely used strategy in human-machine interaction, is to detect forces or movements acting between wearer and device.

The paradigms that use this approach are called *mechanically intrinsic* [8], as they relay on mechanical manifestations of human movements, acquired by sensors on the robot itself; these data are successively fed back into a biomechanical model of the assisted limb to provide the resulting computation to the actuation stage. Common strategies include sensing joint positions, velocities or interaction forces to initiate or modulate the assistance. Mechanically intrinsic controllers are well studied and robust. However, they suffer from two major limitations: (1) being triggered by the outcomes of human intention, they suffer from a time lag between the initiation and detection of movement, with a consequent upper bound on the quality of assistance; (2) when designing a control law for mechanically intrinsic controllers, it is required to make assumptions about the interaction dynamics between the robot and the environment, if such assumptions are wrong, the controller will not perform as intended. A typical example is a controller for gravity-compensation of the arm: the control laws will not compensate for the mass of an object picked up by the human agent.

A solution to these restrictions is possible if we tap into the human nervous system: the control signal generated by the brain to activate muscles, precedes the movement and continuously adapts to environmental dynamics, reflecting the remarkable sensing and planning capabilities of our nervous system. Proportional myoelectric controllers, for example, sense efferent control potentials to provide assistive forces that are proportional to the user's muscle recruitment [9], [10], [11], [12], [13]. Since electromyographic signals (EMG) are produced before the initiation of the movement [14], the robot is more likely to match the movement timing of the user. Even better performance is achieved combining EMG detection with an accurate model of the musculoskeletal geometry and subject-specific activation dynamics, called "*myoprocessor*" [15]. It has been demonstrated that the choice of a *myoprocessor* results in the most robust and reliable solution across all the EMG-driven control frameworks, as elegantly discussed by Sartori and Sawicki [16]. A proportional EMG controller, solely relying on processed EMG signals, does not capture complex aspects related to the dynamics of human biomechanics, since it neglects the muscle geometry contribution and EMG to muscle activation conversion. In [17] Sartori showed that a myoprocessor, relying on muscular geometry as well as activation levels, is able to reject mechanically induced movement artefacts in the EMG signals, such as arm positions, and motion artifact from electrodes and cables.

Despite these theoretical advantages, there is lack of empirical evidence on how humans respond to different intention-detection strategies, implemented on similar or comparable devices and across a wide range of motion dynamics [18]. This makes it hard to speculate if an EMG-based approach would result in a more effective synchronization with the human counterpart, than a mechanically intrinsic paradigm. A work in this direction has been done by Cain and colleagues [19]. The authors showed that a proportional myoelectric controller, implemented on a powered ankle-foot orthosis for walking assistance, results in larger reductions of muscular activation and more physiological gait kinematics than a footswitch-based one. However, the study compared a proportional approach, where the amplitude of the muscular activity modulated the delivered assistance, with a discrete one, where the switch was used to trigger a constant actuation force. Moreover, it is unclear if these results can be generalized to the upper limbs, where the variability of movements and tasks manifold are wider and more unpredictable than in walking.

In our recent work, we proposed, for the first time, an EMG-based approach to control a tendon-driven exosuit through a musculoskeletal model that mapped EMG activation patterns and joint kinematics into joint torque [20]. In a separate and previous contribution, a similar device was also tested with a mechanically intrinsic controller that sensed the interaction force at the pHRI to initiate movement and compensate for gravitational forces [21], [22].

In this work, we propose a comparison between controllers that represent the two main approaches for intention-detection in upper limb wearable robotics: a mechanically intrinsic controller to compensate for inertial and gravity-dependent dynamics (*dynamic arm module*) and a model-based EMG controller (*myoprocessor module*). Our objective is to highlight the pros and cons of each approach and explore the performance of the controllers across different motion dynamics.

We hypothesize that the *myoprocessor*, by tapping into the information carried by the efferent motor commands, will result in better-timed assistive profiles and, unlike the mechanically-intrinsic one, will adapt to changing external dynamics. On the other side, we expect more stability when the exosuit is driven by the *dynamic arm* controller, since we avoid the variability given by the inclusion of biosignals in the loop. To achieve this goal, we evaluated the performance of both controllers on a sample of eight participants while they performed functional tasks, representative of daily living activities, and ballistic tasks (throwing/catching a ball), where the promptness of the assistance plays a prominent role.

II. Hardware and setup

We tested the performance of both real-time control frameworks using our latest fully embedded elbow exosuit (Fig. 1). The device consisted of a textile harness derived from a passive orthosis (Sporlastic Neurolux II, Nürtingen, Germany). The actuation stage, the control architecture and the battery pack were attached to a customized support placed on a motorbike back protector (Zandoná Evo X6, Treviso, Italy). The actuation stage consisted of a brushless DC motor (Maxon EC-i 40, $70\,\mathrm{W}$, Sachseln, Switzerland), in series with a planetary gearhead (Maxon GP32, $\varnothing 32\,\mathrm{mm}$ $51:1$, Sachseln, Switzerland) driving a pulley ($\varnothing 28\,\mathrm{mm}$) around which the suit tendon was wound. The motor axis angular position was measured with an incremental encoder (Scancon 2RMHF, 5000 pulses/rev, Hillerød, Denmark).

A Bowden cable was used to transfer mechanical power, from the actuation to the suit. Torque was provided by the suit to the wearer via two anchor points, located on the proximal

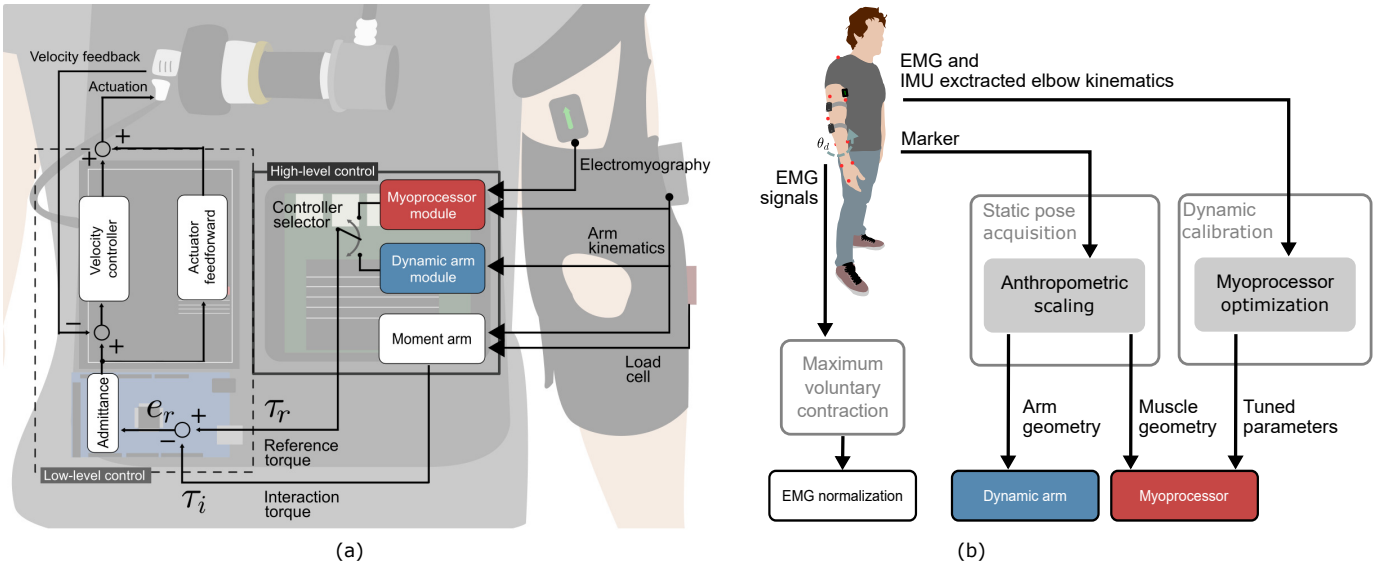

Fig. 2. *Real-time control frameworks and calibration pipeline*. (a) We measured the performance of two different high-level control algorithms: the *myoprocessor module* (red block) estimated the elbow joint torque generated by the muscles through an accurate musculoskeletal model; the *dynamic arm module* (blue block) extracted the arm dynamics effort via inverse dynamics approach, by means of IMUs kinematics and orientation. The model reference torque τ_r was compared to the human-robot interaction torque τ_i acquired from the force sensor placed at the distal anchor point. The torque tracking error e_r was the low-level controller input. This error was then converted into a motor velocity, delivering assistance to the wearer. (b) The high-level controllers calibration consisted of three steps: maximum voluntary contraction trials for EMG normalization, a static pose acquisition that extracted the subject's anthropometry and the dynamic calibration for the parameters tuning of the *myoprocessor*.

and distal sides of the elbow joint. The Bowden cable sheath (Shimano SLR, $\varnothing 5\,\mathrm{mm}$, Sakai, Ōsaka, Japan) was attached to the proximal anchor point, while the tendon (Black Braided Kevlar Fiber, KT5703-06, $2.2\,\mathrm{kN}$ max load, Loma Linda CA, USA) was connected to a force sensor (Futek, FSH04416, Irvine CA, USA) anchored to the distal anchor point. The device also features two inertial measurement units (IMUs, Bosch, BNO055, Gerlingen, Germany), fixed on the orthosis with velcro straps, at the level of the humerus and the ulna to detect the 3D kinematics and orientation of the assisted arm. The overall weight of the device is $3.5\,\mathrm{kg}$ and the battery ($3300\,\mathrm{mA}$) life is $\approx 16\,\mathrm{h}$ of continuous use.

A multi-channel and wireless surface EMG system (Delsys Trigno, Natick MA, USA) was used to monitor six muscles on the right arm: the long head of biceps brachii, the long head of triceps brachii, anterior and posterior parts of the deltoid, the trapezius and the pectoralis major: electrodes placement followed the SENIAM guidelines [23]. The envelope of the EMG signals was directly extracted from the sensor built-in hardware filter (step 1: Butterworth bandpass, 2 pole high pass corner at $20\,\mathrm{Hz}$ and 4 pole low pass corner at $450\,\mathrm{Hz}$; step 2: root mean square envelope on a $100\,\mathrm{ms}$ window), and successively normalized by the individual maximum voluntary contraction (MVC).

We used an Arduino Mega 2560 (Arduino, Ivrea, Italy) as embedded acquisition board placed on the back protector to acquire in real-time the force sensor and the IMUs signals and to send the control command to the motor drive, with a sampling frequency of $1\,\mathrm{kHz}$. The exosuit actuation was driven by a dedicated servo controller (EPOS2 50/5, Maxon, Sachseln, Switzerland) closing an internal feedforward + feedback velocity loop at $1\,\mathrm{kHz}$. The real-time control and data logging was implemented in a MATLAB/Simulink application (MathWorks, Natick, Massachusetts MA, USA), and ran on an embedded computer at $500\,\mathrm{Hz}$ (NVIDIA Jetson Nano, Santa Clara CA, USA), that also took care of the EMG acquisition, via a TCP/IP protocol. The Jetson Nano communicated with the Arduino via a serial bus.

We estimated the human kinematics by recording 12 reflective markers positioned on anatomical landmarks (Qualisys 5+, Göteborg, Sweden): third metacarpus, ulnar styloid, radial styloid, forearm front, forearm back, lateral epicondyle, medial epicondyle, upper arm front, upper arm back, upperarm lateral, acromion and processus spinosus 7^{th} cervical vertebra: the motion capture system ran on a dedicated desktop workstation at $150\,\mathrm{Hz}$.

III. Real-time controllers

In the present work we specifically aimed at comparing the performance of the two main different state of the art controllers, typically used in wearable robotics. The difference between the two controllers consisted of the "*modules*" (Fig. 2a) used for detection of the user's motion intention and computation of the assistance:

- the *myoprocessor module* merges EMG activity to estimated musculoskeleteal dynamics to compute the elbow torque;
- the *dynamic arm module* relied only on a subject specific upper limb biomechanical model to estimate the same torque at the elbow.

For sake of clarity, the aforementioned modules worked non synchronously, meaning that one module excluded the other

while working and computing the assistance, hence they were tested separately and across distinct trials.

As depicted in Fig. 2a, the architecture comprised a high-level controller, including either one of the two modules (selected prior test initiation) which estimated the *assistive reference torque* (τ_r). A low-level admittance controller, common to both the modules, was implemented to track the reference signal.

A. High-level controller: myoprocessor module

The myoprocessor module, already presented in [24], used a musculoskeletal model to compute elbow flexion-extension torque as a function of the muscle activation level and joint angle. Muscular activation was measured with two EMG channels on the biceps brachii and the triceps brachii while joint angles were estimated from the IMUs. The myoprocessor comprised four core modules, as described in details as follows.

1) The activation dynamics: block converts the normalized EMG input of the j-muscle, u_j, into muscle activation a_j via a non-linear transfer function [25]:

$$a_j(t) = \frac{e^{A_j u_j(t)} - 1}{e^{A_j} - 1}. \tag{1}$$

where A_j is a muscle-dependent shape factor that models the fiber recruitment (i.e. EMG-to-activation coefficient).

2) The Muscle-Tendon Unit (MTU) kinematics: models the 3D musculoskeletal geometry (i.e. muscle tendon length l^{mt} and moment arm r^{mt}) of the human arm extracted from Opensim models [26] by means of a set of multidimensional cubic B-splines [27].

3) The MTU dynamics: module estimates the muscle force starting from the *Activation dynamics* and *MTU kinematics* outputs. The force $F_j^{mt}(t)$ produced by the j-muscle was obtained by the equation:

$$F_j^{mt}(t) = F_j^{max}[a_j(t) f_l(t) f_v(t) + f_p(t)] \cdot \cos\phi_j(t) \tag{2}$$

where F_j^{max} is the maximum isometric force [28], $a_j(t)$ the muscle activation, $f_l(t)$, $f_v(t)$ and $f_p(t)$ are respectively the force-length relationship, the force-velocity relationship and the parallel passive elastic muscle force. These functions depend on the muscle fiber length and muscle fiber contraction velocity normalized with respect to the optimal fiber length l_0^m. At last, ϕ_j was the pennation angle of the fibers. The force-length ($f_l(t)$) and the force-velocity ($f_v(t)$) relationships account for the contractile element of the muscle: the first one is represented by a Gaussian function that describes the dependence of the steady-state isometric force of a muscle as a function of muscle length [29]. The force-velocity relationship ($f_v(t)$) is the characteristic dynamic response of the muscle fibers during the contraction [30]. The parallel passive elastic muscle force ($f_p(t)$) describes the behaviour of muscular passive elements and characterized by an exponential relationship, which allows to compute the passive forces regardless of fibre length, and thus accounting for non-zero passive forces [31]. Tendons were assumed to be non-deformable, i.e. with a constant length $l^t(t) = l_s^t$ and the muscle fiber length during movements is always equal to $l^m(t) = l^{mt}(t) - l_s^t$.

4) Torque computation: The last core module combined the muscle forces $F^{mt}(t)$ and the vector $J^{mt}(t)$ of muscle moment arms r^{mt} to estimate the reference torque at the elbow $\tau_r(t)$: this value is the reference input for the low-level controller.

$$\tau_r(t) = J^{mt}(t)^T \cdot F^{mt}(t) \tag{3}$$

B. High-level controller: dynamic arm module

The second control framework, alternative to the myoprocessor, computes the reference torque $\tau_r(t)$ from a biomechanical model of the arm, accounting for the 3D orientation of the joints (i.e. elbow and shoulder) and including inertial, centrifugal, Coriolis and gravitational forces. We adopted the classical equation of motion to compute torque at the joints τ^h and used the component at the elbow to close the loop of the controller [32]:

$$\tau^h(q(t)) = M(q(t))\ddot{q}(t) + C(q(t), \dot{q}(t)) + G(q(t)), \tag{4}$$

where q, $\dot{q}$ and $\ddot{q}$ represent the vectors of elbow and shoulder position, velocity and acceleration, respectively, obtained by means of the IMUs signals. The inertial and mass properties of the arm are described by the matrix $M(q(t))$, $C(q(t), \dot{q}(t))$ is the vector of Coriolis and centrifugal forces and $G(q(t))$ is the vector of gravitational force, extracted from the Opensim musculoskeletal model [26] and scaled on subject anthropometry. The reference torque τ_r is the element of the vector τ^h corresponding to the elbow flexion and extension.

C. Low-level controller: torque and velocity loops

The reference torque $\tau_r(t)$, estimated from the high-level controller, was used as input signal for the low-level admittance controller. The admittance controller compared $\tau_r(t)$ with the interaction torque, $\tau_i(t)$ estimated from the force sensor recording the tendon tension [24]. The resulting instantaneous torque tracking error $e_r = \tau_r - \tau_i$ was transformed into a desired angular velocity, ω_r, through a PID-like admittance block of the form:

$$Y(s) = \frac{\omega_r}{e_r} = \frac{K_p + K_i \cdot s^{-1}}{1 + K_d \cdot s} \tag{5}$$

where the K_p, K_i and K_d gains were experimentally tuned, using the Ziegler-Nichols heuristic method, prior initiation of the study and then left unchanged for all study participants.

Lastly, an inner velocity loop was included for compensation of the intrinsic non linear exosuit dynamics (backlash, Coulomb and viscous friction) and was tuned to provide a stiff, under-damped response, through a Nichols-Ziegler method [33]. Feed-forward acceleration and velocity terms were added to the feedback, to improve the tracking accuracy and bandwidth of the velocity loop.

D. High-level controllers calibration

Contrarily to the low-level, the high-level controller was subject specific: each participant was enrolled in a calibration phase prior starting the experiment, to tune both high-level modules. It is worth mentioning that calibration of the

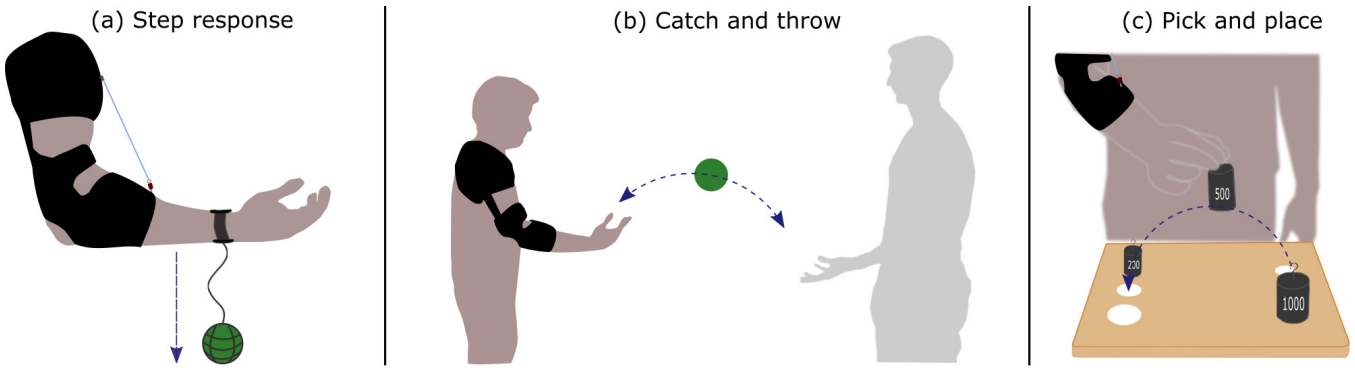

Fig. 3. *Functional tasks*. (a) Human-exosuit response to a step-like external perturbation (i.e. *Step Response* task). (b) *Catch and throw* task with one hand. (c) *Pick and place* task, consisting in grasping and moving objects of different mass to specific target locations.

controllers involved only parameters that were dependent on the participants' anthropometry and physiology, on which both modules rely to evaluate the reference torque $\tau_r(t)$. The calibration step was performed without wearing the exosuit.

The calibration procedure (Fig. 2b) consisted of three different phases: (i) maximum voluntary contraction trials (MVC), (ii) a static pose acquisition, and (iii) a dynamic calibration.

The MVC trials was a series of isometric contractions for each muscle group, used for the EMG-signal normalization and post processing. The static pose consisted of a 30 s rest in the standard anatomical position (upright, arm extended along the trunk) during which we monitored the position of the markers on the anatomical landmarks defined in Section II. We used the open-source software OpenSim to linearly scale a generic musculoskeletal model [26], and match each participant's arm anthropometry, which was successively used to estimate the muscle-tendon geometry of the *myoprocessor* (i.e. muscle-tendon lengths and moment arms) and bones geometry of the *dynamic arm* modules (i.e. bone lengths, mass, inertial, Coriolis matrices and centre of mass). This model was common to both controllers during the experiments and was further used for post-processing.

The dynamic calibration has been performed to tune only the *myoprocessor*, where baseline EMG data at rest was recorded with the elbow fully extended in vertical position ($0°$) for 20 s. Successively, subjects followed elbow flexion/extension reference trajectories, shown on a screen through a phantom arm moving according to the following periodic waveform.

$$\theta_d(t) = A_0 + A\sin(2\pi f(t)t) \tag{6}$$

with $A_0 = A = 45°$, and $f(t)$ being a step-wise varying frequency in increasing steps of 0.05 Hz, between 0.05 Hz and 0.5 Hz: values were chosen as they correspond to movements with a peak velocity between $12.5°$/s and $150°$/s, respectively, equivalent to 10% and 120% of the speed of the elbow in daily tasks [34]. Each frequency of motion was held for 20 s. During this phase, we recorded the marker positions and used them to extract the human elbow torque $\tau_{id}(t)$ through the OpenSim inverse dynamics tool. The recorded EMG signals and joint angles from the IMUs were then used to calibrate the *myoprocessor*: by using the simulated annealing algorithm [35] we minimized the calibration function $f_{cal}(t)$

$$f_{cal}(t) = \frac{1}{N}\sum_{t=1}^{N}(\tau_{id}(t) - \tau_r(t))^2 \tag{7}$$

where $\tau_r(t)$ was the reference torque estimated by the *myoprocessor*. Through this calibration phase, we optimized the values of the internal model parameters related to muscle-tendon physiology: optimal fiber length l_0^m, tendon slack length l_s^t, maximal isometric force F^{max} and EMG-to-activation coefficients A. The fitting of the parameters was performed by setting the physiological bounds, following the procedure and guidelines described in [36].

IV. Experiments

Eight healthy participants were enrolled in the experiment (4 males/4 females, age 26.88 ± 3.72 years, mean $\pm$ SD, body weight 79.63 ± 16.18 kg and height 1.79 ± 0.10 m). Inclusion criteria were based on no evidence or known history of musculoskeletal or neurological diseases, and exhibiting normal joint range of motion and muscle strength.

All experimental procedures were carried out in accordance with the Declaration of Helsinki on research involving human subjects and were approved by the IRB of Heidelberg University (Nr. S-311/2020). All subjects provided explicit written consent to participate in the study. The study consisted in repeated-measurements, where participants, wearing the exosuit, performed three functional tasks in different conditions with and without exosuit assistance (Fig. 3). Each task was performed in all of the three following conditions: "*no assistance*", where the exosuit was worn but unpowered; "*myoprocessor*", where the exosuit was powered and controlled using the EMG-driven musculoskeletal model; "*dynamic arm*", where the exosuit was powered and controlled using the dynamic model of the human arm. The experiment was designed to test the controllers for response time, rejection of external disturbances and adaptation to varying external dynamics. The tasks were named as follows:

A. Step response;
B. Catch and throw;

C. Pick and place.

The whole experiment required three days: the calibration procedure was performed on the first day while the tasks were carried out during the other two days, except for the MVC trial that was executed prior each experimental session. The order of the tasks and conditions was randomized across subjects and days; to avoid onset of muscular fatigue, participants rested for $10\,\mathrm{min}$ between the tasks. Before starting, participants performed a $5\,\mathrm{min}$ familiarisation phase with both control approaches to get accustomed to use the device, performing free movements. Subjects had no information on which controller the device was used during the task with the exosuit (i.e. *myoprocessor*, *dynamic arm*), but were only instructed on how to perform the task.

A. Step response

The *step response* task (Fig. 3a) was designed to evaluate response time and stability of the human-exosuit system to a sudden unexpected external perturbation. Instructed to hold the elbow in a $90°$ flexion, participants were blindfolded in order to prevent any anticipatory action and keep perturbation unpredictable. A medicine ball of $1.36\,\mathrm{kg}$ of mass and $\varnothing\ 10\,\mathrm{cm}$ was attached to the participants' wrist by a non extendable nylon cable. The task initiated once the experimenter released the ball, letting it fall under the effect of gravity, to generate a quasi instantaneous load application at the subject's limb. The sequence was repeated 5 times on each participant.

B. Catch and throw

During the *catch and throw* task (Fig. 3b), participants interacted with a human assistant to perform an exercise consisting of catching and throwing a medicine ball ($1.36\,\mathrm{kg}$ of mass and $\varnothing\ 10\,\mathrm{cm}$). The goal was to evaluate the performance of the controllers during a highly dynamic task in a controlled environment: distance between participant and collaborator was $2\,\mathrm{m}$, and a third experimenter provided a verbal cue to initiate the test. The human assistant threw the ball to the subject, who, after catching it, had to extend the elbow and wait for a second verbal cue to throw back the ball. The sequence was repeated three times in the three conditions: (1) *no assistance*, in which the exosuit cable was slack and the motor turned off, and with the exosuit assisting its user using the (2) *dynamic arm* module and (3) *myoprocessor* module separately.

C. Pick and place

Participants had to *pick and place* items (Fig. 3c) in order to test the adaptation of the controllers to variable load conditions. We used three different precision weights for the experiment: $200\,\mathrm{g}$, $500\,\mathrm{g}$ and $1000\,\mathrm{g}$. Participants waited for an external audio trigger before moving the weight to the corresponding target location: no kinematic nor timing constraints were specified to complete the task. Each trial comprised of a sequence of three loads, repeated four times for a total of 12 movements.

V. Data analysis

Offline analysis was carried out to evaluate the performance of the *dynamic arm* controller and *myoprocessor*, across the different tasks, compared to the *no assistance* condition. Outcome measures included response time, disturbance rejection and adaptation to varying external dynamics.

A. Response time and disturbance rejection

The *step response* task was used to estimate the system response time and disturbance rejection. The initiation of the physiological reaction to the sudden force application, due to the falling load, was obtained by calculating the EMG onset, as the norm of the derivative of the biceps activity greater than $10\ \%$ of its peak value (i.e. velocity threshold onset [37]). This was compared with the recorded force signals from the force sensor, extracting two performance indexes:

- *System response*: the time difference between the EMG onset and the first negative peak of the interaction torque $\tau_i(t)$, which corresponds to mechanical intervention by the exosuit actuation to counteract the force application.
- *Settling time*: the amount of time elapsed from the EMG onset and the first time point after which the value of the interaction torque ($\tau_i(t)$) settles in an range of $\pm 5\%$ of its final value.

We also evaluated the performance of the two controllers in terms of promptness of assistance intervention, by calculating the computational delay occurring between the EMG bursts recorded from the electrode and the exosuit mechanical action ("*Actuation*", Fig. 2b) in response to the subject's movement intention. Assuming that physiological muscle contraction is followed by the mechanical assistance from the exosuit, the computational delay was detected by looking at the cross-covariance [38] between the biceps brachii activity and the output of the low-level controller velocity command to the motor drive actuation (i.e. "*motor actuation command*").

B. Power consumption

The *catch and throw* task provides information on controllers performance during ballistic movements. We computed the exosuit mechanical power during the throw phase of the *catch and throw* task (P_{exo}) by using the relationship

$$P_{exo} = F_{cable} \cdot v_{cable} \tag{8}$$

where F_{cable} is the cable tension force recorded by the force sensor and v_{cable} is the cable velocity estimated from the motor encoder rotational speed, the gear ratio of its planetary gear-head and the diameter of the pulley. For simplicity, we assumed that the torque from the exosuit was transmitted efficiently to the elbow joint and the power loss due to the deformation of the anchor points was negligible. The total power at the elbow was computed according the formula:

$$P_{total} = \tau_{id} \cdot \omega_{elbow} \tag{9}$$

where τ_{id} is the torque at the elbow level extracted from the Opensim inverse dynamics tool and ω_{elbow} is the elbow angular velocity computed via Opensim inverse kinematics

tool. Both signals were estimated based of the markers data. The contribution from the exosuit wearer to the power P_{human} was then estimated as:

$$P_{human} = P_{total} - P_{exo} \tag{10}$$

The work made by each single actor was computed by integrating power across the time. The exosuit and human works were then normalized with respect to the corresponding total work.

C. Adaptation to external dynamics

The second part of the *catch and throw* analysis targeted the effects of assistance on human physiological motion: to such an extent, we extracted joints inverse kinematics by feeding each subject-specific Opensim model with the collected markers data. Shoulder and elbow range of motion and the peak velocities across conditions were compared (*no assistance*, *dynamic arm* and *myoprocessor*).

During both the *catch and throw* and *pick and place* tests, offline computation of the EMG root mean square (RMS) experiment was used as index of muscles activation level.

The *pick and place* task was also useful to evaluate the ability of the two control paradigms to adapt to changing external dynamics. The outcome measure consisted of a comparison between the interaction torque ($\tau_i(t)$) measured by the force sensor and the biological human torque ($\tau_{id}(t)$), extracted in the *no assistance* condition using the Opensim inverse dynamics toolkit and the markers data.

D. Statistical analysis

Data normality distribution was assessed using Shapiro-Wilk test, and sphericity condition for repeated measures analyses of variance (rANOVA) was evaluated using the Mauchly test. A repeated measures ANOVA test was used to examine the effects, on the dependent variables (rms_{ct}) of the type of assistance, using as within-subject factor the rms_{ct} (3 levels: *no assistance*, *dynamic arm*, *myoprocessor*). A post-hoc analysis was performed using paired t-tests to evaluate the significant pairwise differences between each type of assistance. For all the tests, the level of statistical significance was set at 0.05, except for post-hoc analysis, where the significance level was chosen according to the Bonferroni correction for multiple comparisons. Statistical analysis was conducted by using IBM SPSS Statistics 23 (IBM, Armonk, New York, USA).

VI. Results

A. Promptness or stability?

The latency between the user's motor command (EMG onset) and the exosuit assistance onset provides a characterization of the controller performance in terms of response time: shorter is the time delay, better the machine moves in concert with the human. We assessed this aspect, by observing in the *step response* task, how and when the system assisted the user against external perturbation. Fig. 4a shows a double axes plot depicting the level of synchronization between EMG signal and the correspondent controllers motor actuation command. The cross-covariance between the two signals reported a value, for this participant, of $153\,\mathrm{ms}$ for the *dynamic arm* module and $63\,\mathrm{ms}$ for the *myoprocessor* module.

The same analysis across all subjects is reported in Fig. 4b, where the computational delay for the *dynamic arm* resulted to be $147.86\pm4.95\,\mathrm{ms}$ (mean $\pm$ SE). The *myoprocessor* computational delay was $60.71\pm6.46\,\mathrm{ms}$. The statistical analysis highlights a significant difference between the two modules where the *myoprocessor* clearly responded faster than the *dynamic arm module* ($p < 0.001$). Furthermore, the *myoprocessor* computational delay is comparable to the biological time delay between the onset of EMG activity and the mechanical manifestation of muscle contraction for the upper limb (i.e. electromechanical delay), which is $55.5\,\mathrm{ms}$ according to the literature [39]. The computational delay is also reflected into the overall mechanical exosuit response: Fig. 4c displays the biceps activity, the reference torque ($\tau_r(t)$) and the interaction torque ($\tau_i(t)$) for a representative subject, averaged between the 5 repetitions. When the arm is suddenly perturbed by the falling load, the biceps contracts to counteract the external torque (Fig. 4c, EMG peak on top plot), and at the same instant a first peak of force is registered by the force sensor, as shown in the plot of the interaction torque ($\tau_i(t)$) for both control modules (blue and red peaks).

The reaction of the controller modules is delayed, and it is visible as first negative peak in the interaction torque ($\tau_i(t)$), indicated on the plots as "response". From an accurate observation, the *myoprocessor* module seems to be faster in the response than the *dynamic arm* module.

This result is further confirmed by the reference torque ($\tau_r(t)$), which represents the evaluated assistance output from the modules, and it seems to clearly differ between controllers: in fact while the *myoprocessor*, consequently to the load application, promptly reacts with an assistance $\tau_r(t)$ and a clear control effort peak is visible, the *dynamic arm* module seems not able to discriminate between voluntary motion and the perturbation, showing a $\tau_r(t)$ flat and visibly of opposite sign compared to the action of the *myoprocessor*. This phenomenon is also explained by the EMG activity on the top plot, where the muscular activation for the dynamic arm module is higher than the one for the *myoprocessor* module, meaning that the wearer is compensating differently for the external perturbation. Concerning the capacity of the two modules to promptly stabilize after the external disturbance, we found that even if the *dynamic arm* is slower to react, the exclusion of biosignals from the control framework makes the reference torque more stable and, consequently, the control algorithm smoothly drives the interaction torque, stabilizing the system faster than the *myoprocessor* (Fig. 4c, settling times).

These outcomes were statistically confirmed at the population level: Fig. 4d and Fig. 4e show a significant difference between controller modules for both evaluated indexes of time response and settling time: the system response time ($p < 0.001$) was $0.378\pm0.006\,\mathrm{s}$ for the *dynamic arm* and $0.326\pm0.010\,\mathrm{s}$ for the *myoprocessor*. The settling time ($p < 0.001$) was $1.411\pm0.060\,\mathrm{s}$ for the *dynamic arm* and $1.908\pm0.053\,\mathrm{s}$ for the *myoprocessor*.

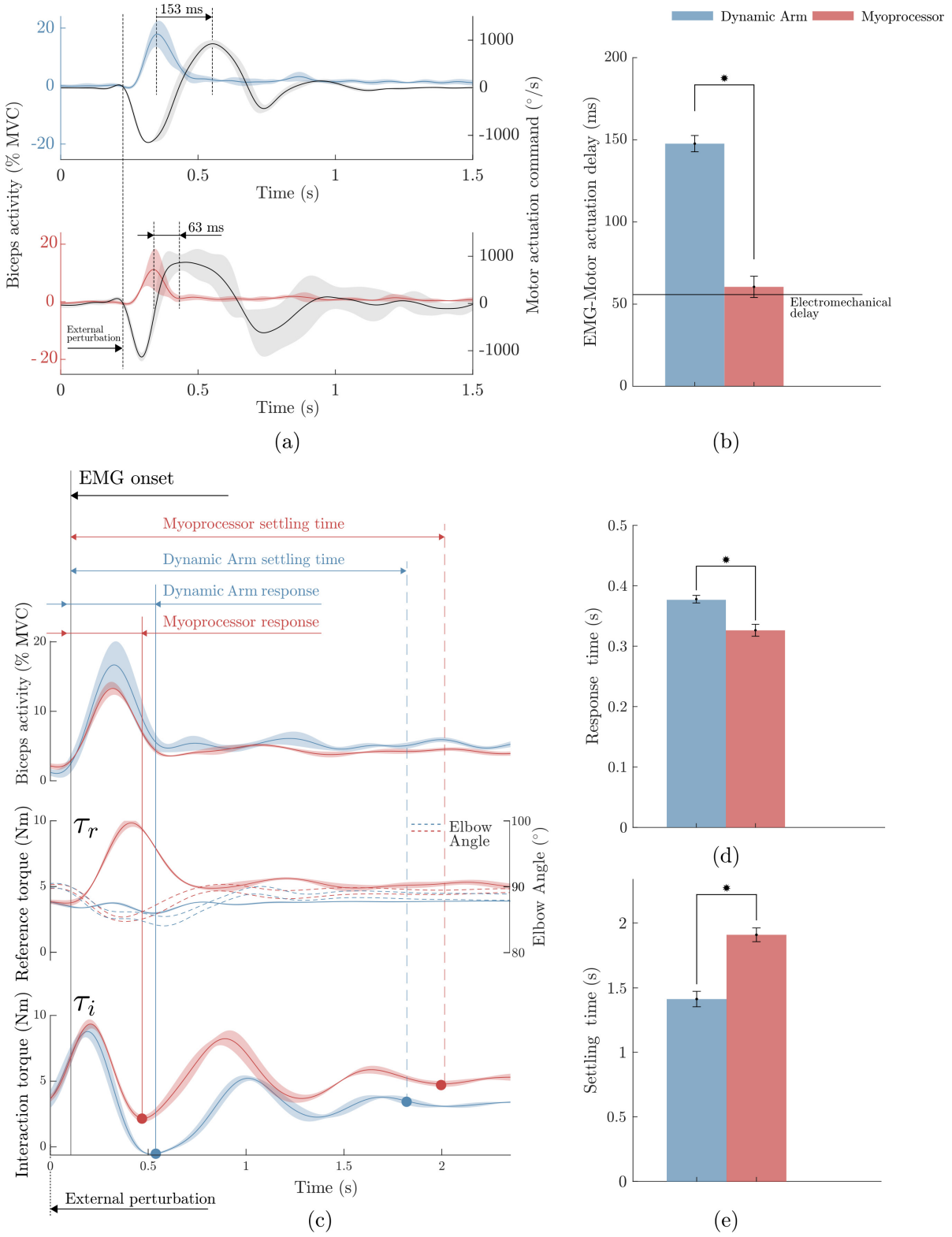

Fig. 4. *Step response: controller response*. (a) Biceps EMG signals of a typical subject with *dynamic arm* (blue line) and the *myoprocessor* (red line) acquired from the EMG probe. The black line represents the motor actuation command. Shaded areas show the standard deviation around the average. (b) Overall computational delay between the biceps EMG signal and the motor actuation at the population level (red and blue bars) compared to the biological electromechanical delay (black line, 55.5 ms). (c) Biceps activity, reference torque, elbow trajectories and interaction torque of a representative subject. Response time (d) and settling time (e) across all subjects.

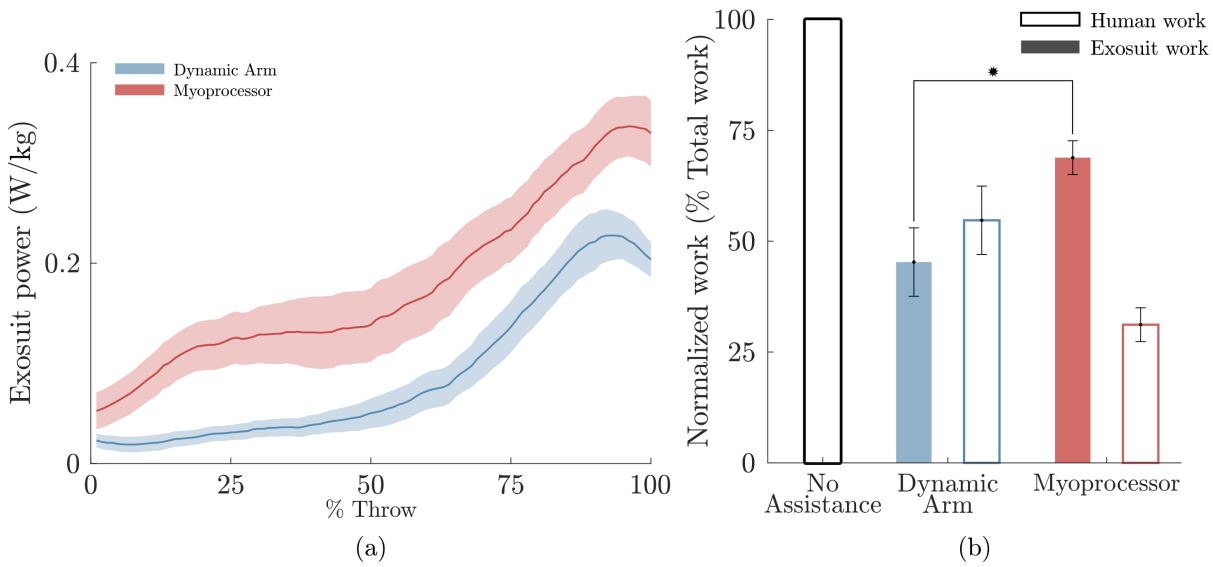

Fig. 5. *Catch and throw: Power analysis*. (a) Exosuit powers across all subjects during the ball throw with the *dynamic arm* assistance (blue line) and *myoprocessor* assistance (red line). (b) Normalized human and exosuit work with respect to the total work.

B. Wearers consumes less energy with the myoprocessor

Curves of generated exosuit power are depicted in Fig. 5a, where a quick visual inspection allows to readily extract few clear differences between the *myoprocessor* and the *dynamic arm* modules: during the ball throw, the device generates more power with the *myoprocessor* controller, instantaneously reacting to the requested assistance. The *dynamic arm*, instead, increase its power around the 25% of the movement and the maximum power peak remains below the *myoprocessor* curve. These results are reflected in the total work: Fig. 5b reports the human and the exosuit mechanical work at the population level, normalized with respect to the corresponding overall work percentage, averaged across subjects in three conditions: without the exosuit (*no assistance*) and with both controllers (*dynamic arm* and *myoprocessor*). During the *dynamic arm* control $45.29 \pm 7.71\%$ of the work was made by the exosuit (mean $\pm$ SE) and $54.71 \pm 7.71\%$ by the human. The situation slightly changed when using the *myoprocessor* module, where exosuit work was $68.84 \pm 3.81\%$ and the human contribution was $31.16 \pm 3.81\%$. The work made by the exosuit resulted in a significant difference between the two controller conditions ($p = 0.002$).

C. Neither controller alters the wearers' kinematics

Fig. 6a displays the human joints trajectory across all participants during the *catch and throw* task, extracted by feeding each subject specific Opensim model with the motion capture data and calculating the inverse kinematics during the *no assistance*, *dynamic arm* and *myoprocessor* conditions. The shoulder flexion time series, shows a reduction of the starting angle during the catching phase (Fig. 6a, top, left) in both the *dynamic arm* and *myoprocessor* conditions: this is due to the exosuit harness that partly limits the joint motion. On the other hand, during the throwing phase, the shoulder trajectories have similar trends across all conditions (Fig. 6a, top, right). The elbow flexion kinematics shows comparable trajectories in the catching phase (Fig. 6a, bottom, left) independently of the conditions. In the final instants of the throwing movement, however, the elbow joint is monotonically flexed when assisted by the exosuit, while it returns to an extended position in the *no assistance* condition. However, as shown in Fig. 6b-c, the statistical analysis at the population level did not result in significant differences in range of motion and peak velocity of the analyzed upper limb joints.

D. Reduction of muscular effort

As a last observation on the *catch and throw* analysis, we evaluated the EMG activation of the main muscles involved during the task execution (Fig. 7): only the biceps brachii showed a significant difference of its activity between the *no assistance* condition and the two controller modules (Assistance effect: $F_{2,14} = 8.100$, $p = 0.005$). Without the exosuit assistance, the biceps RMS was $28.16 \pm 10.36\%$ of the MVC (mean $\pm$ SE); with the *dynamic arm* control, the muscle activity was $23.36 \pm 8.81\%$ and with the *myoprocessor* was $16.89 \pm 7.25\%$. We also reported on Fig. 7b the relative reduction between the *no assistance* condition and the two controller modules, which resulted in about 17% with the *dynamic arm* and 40% for *myoprocessor* in the catching phase. Similar results have been found during the *throw* phase with a reduction of 14% and 32% for the *dynamic arm* and *myoprocessor* assistance respectively. However, statistical analysis of data related to the biceps activity between the *dynamic arm* and the *myoprocessor* conditions did not show significant differences, hence the two controller modules can be considered comparable in terms of performance and reduction of muscular activities during dynamic tasks execution.

We also performed an analysis of muscular activity for the *pick and place* task, in which we computed the RMS for each condition (*no assistance*, *dynamic arm* and *myoprocessor*) and each load (200 g, 500 g and 1000 g) (Fig. 8). We found significant differences between the *no assistance* condition and the *dynamic arm* in the anterior deltoid activity (Assistance

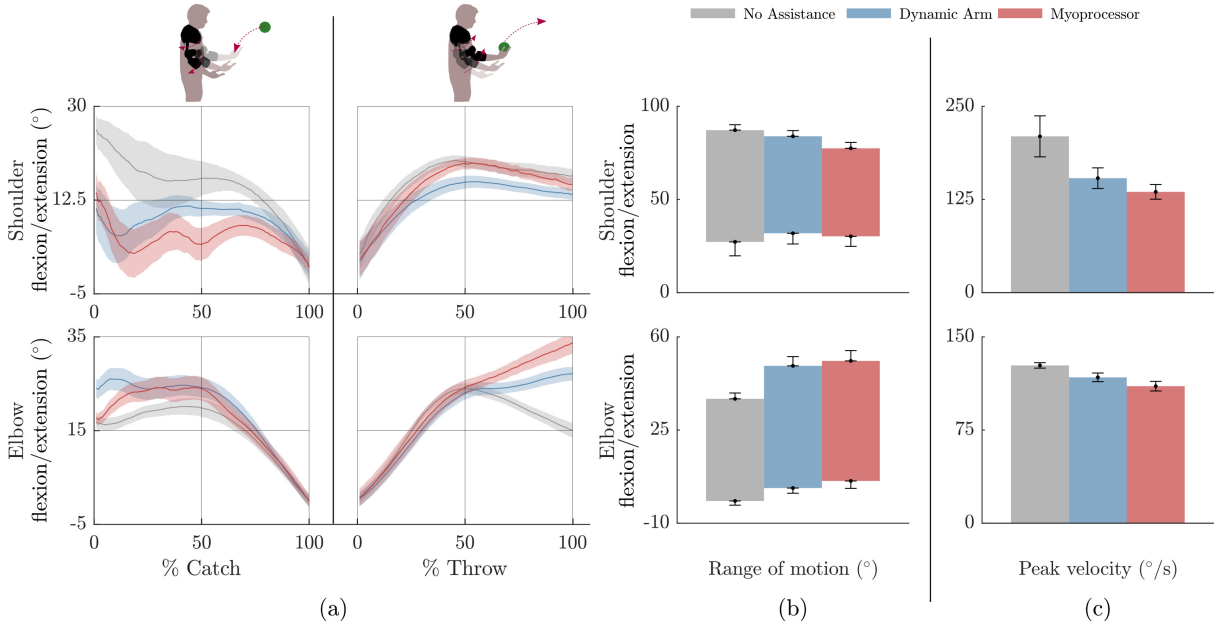

Fig. 6. *Catch and throw: Kinematics*. (a) Joints kinematics across all subjects during the *no assistance* (gray line), *dynamic arm* (blue line) and the *myoprocessor* (red line). Range of motion (b) and peak velocity (c) at the population level.

TABLE I
Pick and place: biceps and anterior deltoid activities.

Biceps activity (% MVC)

200g	6.78 ± 0.67	1.74 ± 0.35	3.02 ± 0.38
500g	7.76 ± 0.67	1.75 ± 0.37	3.20 ± 0.40
1000g	7.46 ± 0.59	1.86 ± 0.34	3.50 ± 0.42

Anterior Deltoid activity (% MVC)

200g	10.21 ± 0.97	8.63 ± 0.51	9.37 ± 0.51
500g	9.69 ± 0.70	7.62 ± 0.42	8.08 ± 0.43
1000g	9.00 ± 0.67	7.37 ± 0.37	8.26 ± 0.42

effect: $F_{2,14} = 8.54$, $p = 0.004$; Load effect: $F_{2,14} = 18.478$, $p < 0.001$; Interaction effect: $F_{4,28} = 4.341$, $p = 0.007$) and, as reported both in Fig. 8b and in Tab. I, across all conditions in the biceps activity (Assistance effect: $F_{2,14} = 6.914$, $p = 0.008$; Load effect: $F_{2,14} = 9.093$, $p = 0.003$). The post-hoc analysis highlighted a significant difference between the *dynamic arm* and the *myoprocessor* across all the three load conditions with reductions of 42%, 45% and 47%, for the 200 g, 500 g and 1000 g respectively.

Also the anterior deltoid showed different activation patterns across loads, as reported in Tab. I, bottom. The post-hoc analysis highlighted the difference between the *no assistance* condition and the *dynamic arm* by lifting 200 g and 500 g (see Fig. 8b).

E. The myoprocessor adapts the assistance to varying dynamics

The use of the two controllers modules allowed also to accurately estimate how the net joint torque at the elbow level was shared between the user and the exosuit during manipulation of different loads, tested during the *pick and place* task. In Fig. 8c-d, we report three torques normalized by the participants' mass:

- the human elbow torque, extracted from the subject specific inverse dynamics model (OpenSim) for the *no assistance* condition.
- the two interaction torques (τ_i), extracted from the exosuit force sensor, for both the *myoprocessor* and the *dynamic arm* modules.

All the values are reported on Tab. II.

TABLE II
Pick and place: measured elbow torque (Nm/kg).

	Inverse dynamics	Interaction torque	
200g	0.43 ± 0.04	0.39 ± 0.08	0.37 ± 0.15
500g	0.59 ± 0.06	0.37 ± 0.08	0.53 ± 0.17
1000g	0.92 ± 0.08	0.38 ± 0.06	0.80 ± 0.22

The statistical analysis across all subjects showed significant difference between the conditions (Load effect: $F_{2,14} = 18.627$, $p < 0.001$; Interaction effect: $F_{4,28} = 20.085$, $p < 0.001$): the post-hoc analysis highlighted significant differences between the *no assistance* and *dynamic arm* torques for the 500 g and 1000 g conditions. We also found significant difference between the *dynamic arm* and *myoprocessor* torques during the maximal load condition, highlighting the capacity of the *myoprocessor* to be able to modulate the assistance depending on the load. Such an effect was not observed during tasks executed in the *dynamic arm* condition.

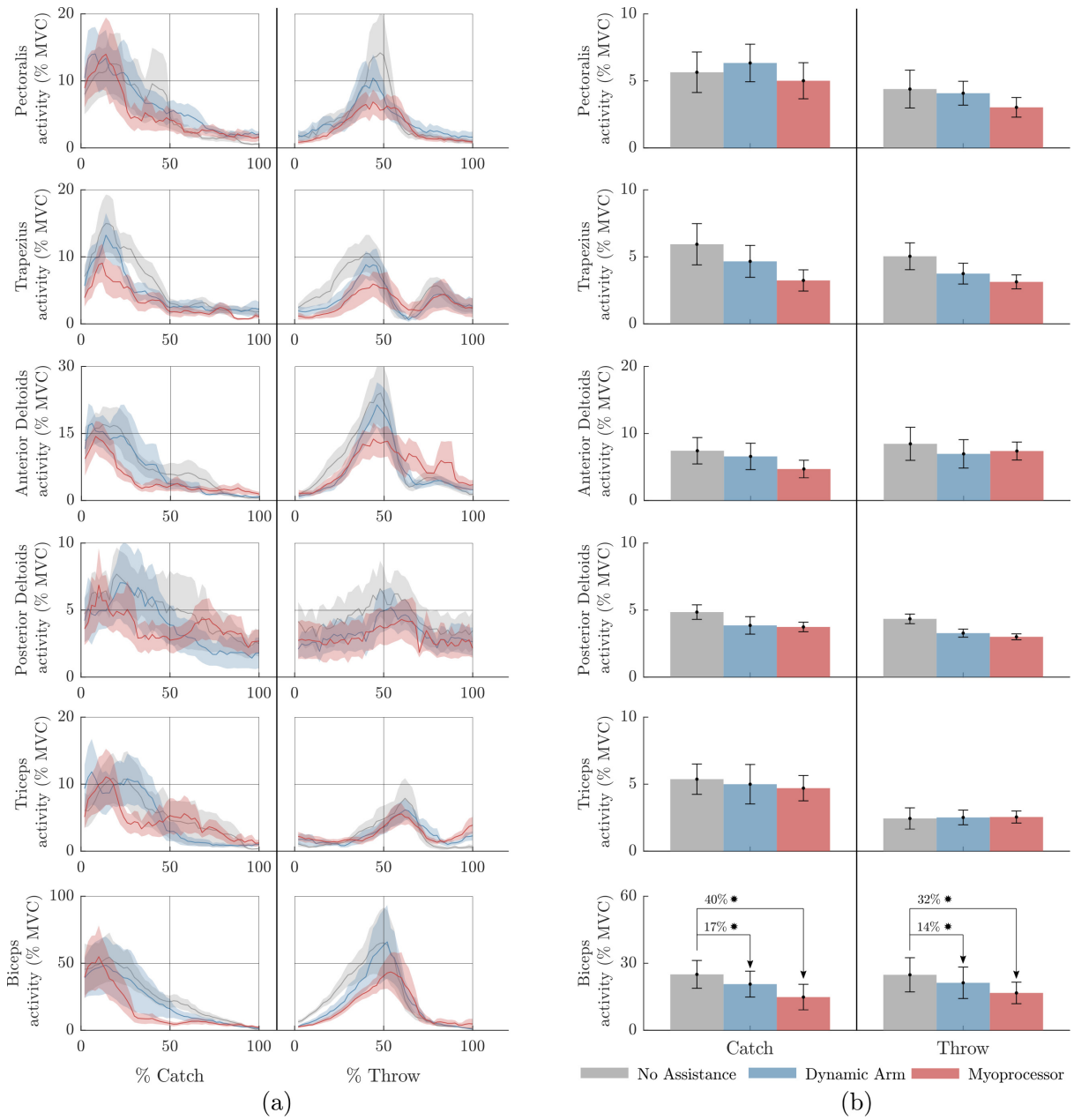

Fig. 7. *Catch and throw: EMG analysis*. (a) Muscular activities across all subjects during the *no assistance* (gray line), *dynamic arm* (blue line) and *myoprocessor* conditions. (b) Muscular activities and EMG reduction at the population level.

VII. Discussion

Ralph Mosher's vision on augmenting wearable technology is better explained in a quote defining his creation as *"...a symbiotic unit with the alacrity of man's information and the control system coupled with the machine's power ruggedness"*.

Aware of the importance of the "alacrity of man's information system", we originally started the investigation in our preliminary work [40] which posed the question on what, between the two main control approaches in human machine interaction, was best to interpret user's motion and robustly control a soft wearable actuated device.

Are biosignals really necessary to synchronize biological and robotic motions, or could wearable devices solely rely on internal interaction forces between the machine and the wearer?

The scope of the current contribution was to provide the reader, not only with two distinctive solutions to efficiently control a soft wearable device, but also to highlight the fundamental differences between them and characterize their performance by proposing a new testing paradigm, across a variety of tasks aiming at replicating functional human interaction with the environment.

A. Synchronization between human and robotic torques

Our first hypothesis was that the myoprocessor would result in assistive force profiles better synchronized to the activity of the biological muscles.

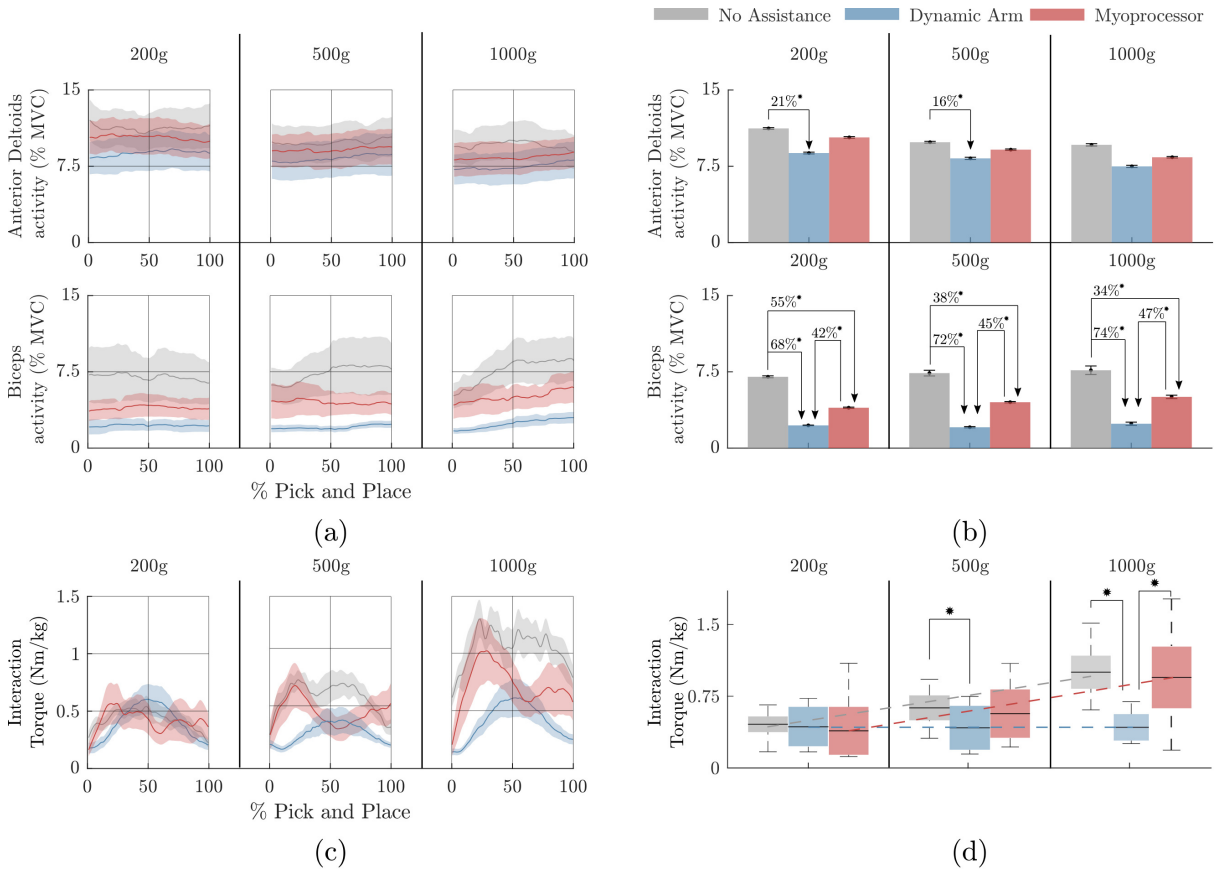

Fig. 8. *Pick and place: changing in muscle activities and interaction torques*. (a) Muscular activity across all subjects during the three different movements of the *pick and place* task. (b) EMG activity barplots at the population level. (c) Elbow joint torque extracted from the inverse dynamic model during the *no assistance* condition (gray line) vs interaction torques under the *dynamic arm* (blue line) and *myoprocessor* assistance for a representative subject. (d) Interaction torques across all participants.

What we found (see Fig. 4b), confirms that an EMG-driven control approach has a shorter computational delay, in responding to the user intention, than a mechanically-intrinsic controller, which does not contemplate biosignals as feedback. A further verification of the high *myoprocessor* promptness comes from the computational time needed for calculating and sending out commands to the actuation unit, which was below the physiological electromechanical delay range (i.e $30-100\,\mathrm{ms}$ [39]). This is, to our knowledge, the fastest implementation approach to fill the time gap between the dynamics of a wearable device and its wearer. The result is comparable to our previous work [20] and to recently published myocontrol techniques [41], [42].

To such an extent, the importance of promptness in dynamic response is paramount in wearable device if one wants to avoid affecting the wearer's sense of agency, which is compromised in presence of a delay between the user's movement intention and the exosuit assistance. In a seminal study on human-machine interaction, dating back to the early days of the field, it has been found that a machine response to the user's action needs to be below $100\,\mathrm{ms}$ in order to be perceived as "real-time" [43]. More recent studies have further shown that even longer time lags between actions and their effects, especially in a time range between 300 and $500\,\mathrm{ms}$, induces a lower sense of agency [44]. This concept applies to the temporal delay between actuator response and human efferent signals: movement intention detection and proprioceptive feedback seem essential to promote intuitive control and body ownership [45]. This assumes a crucial relevance in clinical applications where strong connection between robot and body perception, referred as "embodiment", is a paramount factor for neuromotor recovery [46]. The same concept applies, even with a more significant effect, to other domains of assistive robotics which require higher responsiveness and dynamic matching between the user and the worn device: this is the case of safety/performance augmentation in industrial wearable robotics.

The responsiveness of controller assistance delivery was deeply investigated in the current paper: by testing the two proposed control schemes in a variety of tasks, we quantified their promptness in providing torques when the wearer attempts to move, accurately evaluating the actuation response and comparing it with the physiological electromechanical delay. Our results clearly show that both architectures provided a minimal delay from the onset of user's motion ($147\,\mathrm{ms}$ and $60\,\mathrm{ms}$ for the *dynamic arm* and *myoprocessor*, respectively, Fig. 4b), yet, physiological kinematics was preserved.

B. Versatility in activities of daily living

Our second hypothesis was that the *myoprocessor*, unlike a mechanically-intrinsic controller (*dynamic arm*), would be able to discriminate external disturbances from the wearer's intention, and reject them in order to provide a more robust stability.

In a scenario where a wearable robot supports a human in unstructured daily environments there are more than just two actors. Three entities play their roles and continuously exchange dynamic information: the human, the exosuit and the external environment. Although in the previous section we tried to highlight the importance of detecting users' movement intention and promptly responding with assistance, yet one must consider that, outside of a controlled lab setting, the dualism of a human-exosuit system is immersed and subjected to external action from the environment.
Hence, it is crucial how external dynamics, which may unpredictably perturb user motion, are translated by the controller and rejected in order to discriminate between disturbance and desired input. Outcomes extracted from the "*step response*" experiment, highlighted how both controllers, were able not only to preserve stability but also modulate the assistance to provide comparable settling times and to reduce oscillations after the onset of the external perturbation. On the other side, a further observation extracted from the "*catch and throw*" task provided information on the dynamic bandwidth of the controllers during fast, ballistic movements: we quantitatively analyzed on how abrupt changes of muscular activation, consequent to sudden impact of a heavy object with the wearer biomechanics, are translated into mechanical assistance, and we observed both assisted and unassisted muscular EMG patterns during the task (Fig. 7). Surprisingly, only the assisted degree of freedom (DoF) was influenced in its muscular activation, while the unassisted DoFs preserved their kinematics as well as their EMG patterns, meaning that the device assistance does not disrupt motion synergies also in tasks requiring highly dynamic motions.

The only solution to avoid controller misinterpretations between internal and external dynamics is to include, in its internal feedbacks, the user's neural signals, hence providing the hardware with a sensing network coordinated with the biological counterpart, as previously proposed in [42], [47], [48], [49]. Nevertheless, to our knowledge, no experimental paradigms specifically designed to measure and characterize disturbance rejection performance in controllers for soft wearable robotics, have been ever proposed.

By means of the such approach we have been able to demonstrate that the *myoprocessor* is able to discriminate between external and internal forces, and to successively provide a stabilizing control effort synchronous with the human postural reactions (Fig. 4).

On the other side, the *dynamic arm*, due to the lack of EMG signals in its feedback loop, initially misinterprets the external perturbation working antagonistically to the user's muscles in the initial transient response. Such different performances between modules in transitory responses have been accurately quantified, demonstrating that including EMG in assistance computation allows to better synchronize the actions between the exosuit and the wearer, at the price of a larger computational load due to the additional biosignals sensing, if compared to the mechanically intrinsic controller. Despite the *dynamic arm* module is unable to discriminate between external and internal forces, missing a correct response in the transitory regime, it shows a better capacity in stabilizing the arm posture than the *myoprocessor* (see Fig. 4e) with a difference of $\approx 500\,\mathrm{ms}$. It is worth mentioning that all the participants, blindfolded and without knowledge about what type of controller was driving the exosuit during the task, were not been able to distinguish which of the two control modules was driving the assistance. This is a further confirmation that the controllers have comparable performances and do not outperform each other, but rather present complementary capacities.

C. Reduction in muscular effort

The "*pick and place*" task has been designed as a reinterpretation of motion accuracy tested in robotics trajectory control: in detail, we wonder if during accurate movements, the mutual interaction between the exosuit and the wearer is consistently kept stable and comparable performance are reached independently on variable payloads. Negligible differences in motion accuracy demonstrated that both control architectures are able to smoothly assist human motion without hampering natural kinematics.

It is worth noticing that, the *dynamic arm* significantly reduced the users's muscular activity in a higher percentage if compared to the *myoprocessor* across all the load conditions: yet the relative difference between the two control modules ($\approx 45\%$ in the biceps activity) is due to variability in the assistance provided by the *myoprocessor* that is dictated by the presence of the myosignals in the loop, highly variable depending on the load conditions. In fact, including EMG signals in the assistance computation may results in a variable modulation of the motor command depending on payload: hence for light objects, the action of the *myoprocessor* delivers a lower assistance when compared to the one provided by the *dynamic arm* which is contrarily constant independently on the weight of the object (Fig. 8c-d).

D. Human energy expenditure

The benefit that the user takes from the exosuit regards not only the changes in muscular activity, but consequently the amount of power required to achieve a specific task characterized by a highly dynamic behaviour and involving high motion speeds. We decided to investigate how the two control modules transfer power to the human body during a *catch and throw* task. The *dynamic arm* controller showed a decrease of power with a lower part of the energy required for the task delivered by the exosuit (Fig. 5a). This is due to the non-adaptation at high-speed tasks, resulting in a high energy expenditure of the human counterpart. These results confirmed what we previously found in [21], in which we observed a performance deterioration for increasing movement velocities, when the *dynamic arm* module lacked of responsiveness to

fast kinematics. A further confirmation was provided by the participants that reported a feeling with the *myoprocessor* module, which, contrarily to the previous case, allowed to release power from the wearer and transfer the major part of the effort to the exosuit actuation, demonstrating how in case of quick motion and prompt assistance delivery the *myoprocessor* outruns the *dynamic arm*.

E. Setup time and practical considerations

Calibration is a natural, continuous process which runs in background at the low level of brain motor adaptation when a new dynamics is experienced proprioceptively.

In the wearable robotics field, the wearer and the device need to be both to calibrate to each other and coordinate their actions to efficiently exploit the advantage from a unified parallel dynamic interaction [50]. In the present contribution, we mentioned that both controllers required a subject-specific calibration and share the same modeling layer: however, while the *dynamic arm* needs anthropometric data related to subject's mass and limb geometry for the biomechanical model in the loop, the *myoprocessor* must rely on an additional optimization procedure to fine-tune internal parameters of its composing blocks conditioning the EMG input signals layer. Despite the two calibration procedures are different in terms of time, effort and computation, it is worth to say that the *dynamic arm* offers a simpler and quicker setup process compared to the *myoprocessor*, making the former more suitable for "off the shelf" technology and applications.

For a daily scenario (i.e. assistive technology for industrial settings), the *myoprocessor* calibration pipeline might be considered too complex because it requires availability of dedicated instrumentation and multiple electrodes which may result unpractical and not reliable in a long time usage. In order to solve this issue, previous contributions were focused on developing real-time myoelectric control optimization [51], [52] with the aim of simplifying the initial calibration procedure and avoiding EMG signals degradation (e.g. skin impedance changes and muscular fatigue) to stabilize the performance of the device for a longer use. In the rehabilitation realm, testing controllers is somehow patient dependant in terms of performance to properly compensate the loss of motor functions [53]: both the controllers strongly rely on patient's residual motor functions to generate assistance. Hence, poor EMG activation and/or residual voluntary motion pose a limit to the efficacy of the proposed controllers. However, encouraging results have been reported in mildly impaired patients for both *myoprocessor* [54] and a similar *dynamic arm* approaches [55].

From our perspective, based on the outcomes herewith reported and the comparative tests, we can state that the *myoprocessor* and the *dynamic arm* have complementary features, and can represent viable solutions for distinct task depending applications: for example, if the assistance needs to be modulate in real-time, like lifting different loads, a *myoprocessor*-driven exosuit could provide more benefit to the user who will have an online modulation of the assistance level. On the other hand, if the aim is to move objects within a specified constant range of dynamics, the *dynamic arm* module can provide more stability during the assistance and an extremely more practical setup not involving biosignals in the loop and not necessarily requiring an accurate calibration procedure.

The first limitation of our study is that the exosuit actuated only a single DoF, while it has been demonstrated that assisting a reduced number of joints may results for the other contiguous anatomical articulations in an abnormal muscular activation [56]. Long term effects of exoskeletons/exosuits and related controllers currently represent an open debate which is challenging several disciplines ranging from robotics to neuroergonomics and psychophysiscs. On this last aspect as well, our current contribution lacks of ergonomic tests to validate which between the two controllers has been perceived less intrusive. Yet, to such an extent, we wanted to ask participants if they were able to distinguish between the quality of the two assistances provided by the *myoprocessor* or *dynamic arm*, and surprisingly none of them were able to tell what controller was used. This is also a confirmation of our results on the time response which presented a low difference ($100\,\mathrm{ms}$) between the two controllers.

We may speculate that such relative time delay between controllers intervention might result noticeable for task were high dynamics are requested and the bandwidths of the control modules may play a major role. However, a research paradigm involving questionnaires and tests specifically for assessing human factors is progressively becoming a road map which, in our opinion, is gradually steering the aforementioned multiple disciplines towards a common scope.

Another limitation of our proposed study concerns the nature of the tested cohort of healthy participants, hence the performance of the two control schemes in a clinical setting is still an open question. Further studies should focus on testing such performances on neurological patients (e.g. stroke or incomplete spinal cord injury) to clearly demonstrate that such approaches can be considered a viable option and concretely impact wearable assistive technology. The main target of our contribution was to provide the community with a new experimental paradigm to test controllers in soft wearable technology, and quantify the intrinsic different behaviours of the two main complementary control paradigms currently in use.

VIII. Conclusions

Despite the two control approaches offer a robust viable option to wearable devices, their working principles result in slightly diverse behaviours: the *myoprocessor* module reliably and promptly detects the user's movement intention, it is able to online adapt the assistance by discriminating external perturbations from wearer's intentions and consequently results in lower muscular effort when dynamically delivering power, in comparison to the *dynamic arm* module.

The advantage of using model based myoprocessing techniques comes at a cost: (1) parameters tuning requires a time-consuming calibration procedure; (2) involving biosignals detection in the loop, it intrinsically suffers from sensitivity

to electrodes placement, detachment and changes in skin electrical impedance.

On the other hand, the *dynamic arm* controller has both its strength and weakness in its simplicity: based on a subject specific biomechanical model and processing mechanically intrinsic signals, which are generally not subjected to time degradation, it is reliable on the long run and less sensitive to changes in biosignals' pattern which are widely variable across subjects.

If one envisions a large consumer technology, a ready-to-use solution with a simple and quick setup procedure, as for the *dynamic arm*, has clearly an advantage over the *myoprocessor* especially in term of robustness and stable performance, even if it results in a non-adapting assistance delivery. On the other side, a controller including in the loop myo-signals offer a wider range of robot-aided assistive solutions, contemplating above all clinical applications where patient's motion intention detection, in severe neurological scenarios, can be only interpreted via implementation of control paradigms based on detection of residual biosignals.

ACKNOWLEDGEMENTS

This work was partly supported by the Swiss National Center of Competence in Research (NCCR) Robotics. We acknowledge Sporlastic GmbH for providing us with the materials to build the exosuit and MathWorks for the technical support.

REFERENCES

[1] R. S. Mosher, "Handyman to Hardiman," *SAE Transactions*, vol. 76, no. 1, pp. 588–597, 1967.

[2] M. Xiloyannis, R. Alicea, A.-M. Georgarakis, F. L. Haufe, P. Wolf, L. Masia, and R. Riener, "Soft Robotic Suits: State of the Art, Core Technologies, and Open Challenges," *IEEE Transactions on Robotics*, pp. 1–20, 2021.

[3] J. L. Pons, *Wearable robots: biomechatronic exoskeletons*. John Wiley & Sons, 2008.

[4] A. T. Asbeck, S. M. De Rossi, I. Galiana, Y. Ding, and C. J. Walsh, "Stronger, smarter, softer: Next-generation wearable robots," *IEEE Robotics and Automation Magazine*, vol. 21, no. 4, pp. 22–33, 2014.

[5] A. Schiele and F. C. Van Der Helm, "Kinematic design to improve ergonomics in human machine interaction," *IEEE Transactions on neural systems and rehabilitation engineering*, vol. 14, no. 4, pp. 456–469, 2006.

[6] J. Kim, G. Lee, R. Heimgartner, D. A. Revi, N. Karavas, D. Nathanson, I. Galiana, A. Eckert-Erdheim, P. Murphy, D. Perry *et al.*, "Reducing the metabolic rate of walking and running with a versatile, portable exosuit," *Science*, vol. 365, no. 6454, pp. 668–672, 2019.

[7] C. T. O'Neill, T. Proietti, K. Nuckols, M. E. Clarke, C. J. Hohimer, A. Cloutier, D. J. Lin, and C. J. Walsh, "Inflatable soft wearable robot for reducing therapist fatigue during upper extremity rehabilitation in severe stroke," *IEEE Robotics and Automation Letters*, 2020.

[8] J. R. Koller, D. A. Jacobs, D. P. Ferris, and C. D. Remy, "Learning to walk with an adaptive gain proportional myoelectric controller for a robotic ankle exoskeleton," *Journal of NeuroEngineering and Rehabilitation*, vol. 12, no. 1, pp. 1–14, nov 2015. [Online]. Available: http://dx.doi.org/10.1186/s12984-015-0086-5

[9] A. Fougner, O. Stavdahl, P. J. Kyberd, Y. G. Losier, and P. A. Parker, "Control of upper limb prostheses: Terminology and proportional myoelectric controla review," *IEEE Transactions on Neural Systems and Rehabilitation Engineering*, 2012.

[10] N. Jiang, T. Lorrain, and D. Farina, "A state-based, proportional myoelectric control method: online validation and comparison with the clinical state-of-the-art," *Journal of neuroengineering and rehabilitation*, vol. 11, no. 1, pp. 1–11, 2014.

[11] A. Ebied, E. Kinney-Lang, and J. Escudero, "Higher order tensor decomposition for proportional myoelectric control based on muscle synergies," *Biomedical Signal Processing and Control*, vol. 67, p. 102523, 2021.

[12] J. R. Koller, D. A. Jacobs, D. P. Ferris, and C. D. Remy, "Learning to walk with an adaptive gain proportional myoelectric controller for a robotic ankle exoskeleton," *Journal of neuroengineering and rehabilitation*, vol. 12, no. 1, pp. 1–14, 2015.

[13] A. J. Young, H. Gannon, and D. P. Ferris, "A biomechanical comparison of proportional electromyography control to biological torque control using a powered hip exoskeleton," *Frontiers in bioengineering and biotechnology*, vol. 5, p. 37, 2017.

[14] R. Merletti and P. Parker, *Electromyography : physiology, engineering, and noninvasive applications*, 11th ed. Wiley-IEEE Press, 2004.

[15] M. Sartori, M. Reggiani, D. Farina, and D. G. Lloyd, "EMG-Driven Forward-Dynamic Estimation of Muscle Force and Joint Moment about Multiple Degrees of Freedom in the Human Lower Extremity," *PLoS ONE*, 2012.

[16] M. Sartori and G. S. Sawicki, "Closing the loop between wearable technology and human biology: A new paradigm for steering neuromuscular form and function," *Progress in Biomedical Engineering*, vol. 3, no. 2, p. 023001, 2021.

[17] M. Sartori, G. Durandau, S. Došen, and D. Farina, "Robust simultaneous myoelectric control of multiple degrees of freedom in wrist-hand prostheses by real-time neuromusculoskeletal modeling," *Journal of Neural Engineering*, vol. 15, no. 6, p. 066026, oct 2018. [Online]. Available: https://doi.org/10.1088%2F1741-2552%2Faae26b

[18] M. Sartori, D. G. Llyod, and D. Farina, "Neural data-driven musculoskeletal modeling for personalized neurorehabilitation technologies," *IEEE Transactions on Biomedical Engineering*, vol. 63, no. 5, pp. 879–893, May 2016.

[19] S. M. Cain, K. E. Gordon, and D. P. Ferris, "Locomotor adaptation to a powered ankle-foot orthosis depends on control method," *Journal of NeuroEngineering and Rehabilitation*, vol. 4, pp. 1–13, 2007.

[20] N. Lotti, M. Xiloyannis, G. Durandau, E. Galofaro, V. Sanguineti, L. Masia, and M. Sartori, "Adaptive model-based myoelectric control for a soft wearable arm exosuit: A new generation of wearable robot control," *IEEE Robotics Automation Magazine*, vol. 27, no. 1, pp. 43–53, 2020.

[21] M. Xiloyannis, D. Chiaradia, A. Frisoli, and L. Masia, "Physiological and kinematic effects of a soft exosuit on arm movements," *Journal of NeuroEngineering and Rehabilitation*, vol. 16, no. 1, p. 29, Feb 2019. [Online]. Available: https://doi.org/10.1186/s12984-019-0495-y

[22] D. Chiaradia, M. Xiloyannis, C. W. Antuvan, A. Frisoli, and L. Masia, "Design and embedded control of a soft elbow exosuit," in *2018 IEEE International Conference on Soft Robotics (RoboSoft)*, April 2018, pp. 565–571.

[23] H. J. Hermens, B. Freriks, C. Disselhorst-Klug, and G. Rau, "Development of recommendations for semg sensors and sensor placement procedures," *Journal of Electromyography and Kinesiology*, vol. 10, no. 5, pp. 361 – 374, 2000.

[24] F. Missiroli, N. Lotti, M. Xiloyannis, L. H. Sloot, R. Riener, and L. Masia, "Relationship between muscular activity and assistance magnitude for a myoelectric model based controlled exosuit," *Frontiers in Robotics and AI*, vol. 7, p. 190, 2020.

[25] D. G. Lloyd and T. F. Besier, "An EMG-driven musculoskeletal model to estimate muscle forces and knee joint moments in vivo," *Journal of biomechanics*, vol. 36, no. 6, pp. 765–776, 2003.

[26] K. R. Holzbaur, W. M. Murray, and S. L. Delp, "A model of the upper extremity for simulating musculoskeletal surgery and analyzing neuromuscular control," *Annals of biomedical engineering*, vol. 33, no. 6, pp. 829–840, 2005.

[27] M. Sartori, M. Reggiani, A. J. van den Bogert, and D. G. Lloyd, "Estimation of musculotendon kinematics in large musculoskeletal models using multidimensional B-splines," *Journal of biomechanics*, vol. 45, no. 3, pp. 595–601, 2012.

[28] F. E. Zajac, "Muscle and tendon: properties, models, scaling, and application to biomechanics and motor control." *Critical reviews in biomedical engineering*, vol. 17, no. 4, pp. 359–411, 1989.

[29] J. M. Winters, "Hill-based muscle models: a systems engineering perspective," in *Multiple muscle systems*. Springer, 1990, pp. 69–93.

[30] B. Katz, "The relation between force and speed in muscular contraction," *The Journal of Physiology*, vol. 96, no. 1, pp. 45–64, 1939.

[31] L. M. Schutte, M. M. Rodgers, F. Zajac, and R. M. Glaser, "Improving the efficacy of electrical stimulation-induced leg cycle ergometry: an analysis based on a dynamic musculoskeletal model," *IEEE Transactions on Rehabilitation Engineering*, vol. 1, no. 2, pp. 109–125, 1993.

[32] M. Katayama and M. Kawato, "Virtual trajectory and stiffness ellipse during multijoint arm movement predicted by neural inverse models," *Biological cybernetics*, vol. 69, no. 5-6, pp. 353–362, 1993.
[33] J. G. Ziegler, N. B. Nichols *et al.*, "Optimum settings for automatic controllers," *trans. ASME*, vol. 64, no. 11, 1942.
[34] M. A. Buckley, A. Yardley, G. R. Johnson, and D. A. Cams, "Dynamics of the upper limb during performance of the tasks of everyday living—a review of the current knowledge base," *Proceedings of the Institution of Mechanical Engineers, Part H: Journal of Engineering in Medicine*, vol. 210, no. 4, pp. 241–247, 1996, pMID: 9046184. [Online]. Available: https://doi.org/10.1243/PIME_PROC_1996_210_420_02
[35] A. Das and B. K. Chakrabarti, *Quantum annealing and related optimization methods*. Springer Science & Business Media, 2005, vol. 679.
[36] G. Durandau, D. Farina, and M. Sartori, "Robust real-time musculoskeletal modeling driven by electromyograms," *IEEE transactions on biomedical engineering*, vol. 65, no. 3, pp. 556–564, 2018.
[37] R. Shadmehr and F. A. Mussa-Ivaldi, "Adaptive representation of dynamics during learning of a motor task," *Journal of Neuroscience*, 1994.
[38] L. A. Zadeh, "Correlation functions and power spectra in variable networks," *Proceedings of the IRE*, vol. 38, no. 11, pp. 1342–1345, 1950.
[39] P. R. Cavanagh and P. V. Komi, "Electromechanical delay in human skeletal muscle under concentric and eccentric contractions," *European journal of applied physiology and occupational physiology*, vol. 42, no. 3, pp. 159–163, 1979.
[40] N. Lotti, M. Xiloyannis, F. Missiroli, D. Chiaradia, A. Frisoli, V. Sanguineti, and L. Masia, "Intention-detection strategies for upper limb exosuits: model-based myoelectric vs dynamic-based control," in *2020 8th IEEE RAS/EMBS International Conference for Biomedical Robotics and Biomechatronics (BioRob)*. IEEE, 2020, pp. 410–415.
[41] R. Leib, M. Russo, A. d'Avella, and I. Nisky, "A bang-bang control model predicts the triphasic muscles activity during hand reaching," *Journal of Neurophysiology*, 2020.
[42] N. Krausz, D. Lamotte, I. Batzianoulis, L. Hargrove, S. Micera, and A. Billard, "Intent prediction based on biomechanical coordination of emg and vision-filtered gaze for end-point control of an arm prosthesis," *IEEE Transactions on Neural Systems and Rehabilitation Engineering*, 2020.
[43] R. B. Miller, "Response time in man-computer conversational transactions," in *Proceedings of the December 9-11, 1968, fall joint computer conference, part I on - AFIPS '68 (Fall, part I)*. San Francisco, California: ACM Press, 1968, p. 267.
[44] W. Wen, A. Yamashita, and H. Asama, "The influence of action-outcome delay and arousal on sense of agency and the intentional binding effect," *Consciousness and Cognition*, 2015.
[45] M. Tsakiris, M. R. Longo, and P. Haggard, "Having a body versus moving your body: Neural signatures of agency and body-ownership," *Neuropsychologia*, 2010.
[46] M. Pazzaglia and M. Molinari, "The embodiment of assistive devices—from wheelchair to exoskeleton," *Physics of Life Reviews*, vol. 16, pp. 163–175, mar 2016.
[47] C. G. McDonald, J. L. Sullivan, T. A. Dennis, and M. K. O'Malley, "A myoelectric control interface for upper-limb robotic rehabilitation following spinal cord injury," *IEEE Transactions on Neural Systems and Rehabilitation Engineering*, vol. 28, no. 4, pp. 978–987, 2020.
[48] E. Trigili, L. Grazi, S. Crea, A. Accogli, J. Carpaneto, S. Micera, N. Vitiello, and A. Panarese, "Detection of movement onset using emg signals for upper-limb exoskeletons in reaching tasks," *Journal of neuroengineering and rehabilitation*, vol. 16, no. 1, p. 45, 2019.
[49] A. Cavallo, A. Koul, C. Ansuini, F. Capozzi, and C. Becchio, "Decoding intentions from movement kinematics," *Scientific Reports*, vol. 6, no. 1, pp. 1–8, 2016.
[50] K. E. Gordon and D. P. Ferris, "Learning to walk with a robotic ankle exoskeleton," *Journal of Biomechanics*, vol. 40, no. 12, pp. 2636–2644, 2007.
[51] M. Couraud, D. Cattaert, F. Paclet, P.-Y. Oudeyer, and A. De Rugy, "Model and experiments to optimize co-adaptation in a simplified myoelectric control system," *Journal of neural engineering*, vol. 15, no. 2, p. 026006, 2018.
[52] C. Nissler, M. Nowak, M. Connan, S. Büttner, J. Vogel, I. Kossyk, Z.-C. Márton, and C. Castellini, "Vita—an everyday virtual reality setup for prosthetics and upper-limb rehabilitation," *Journal of neural engineering*, vol. 16, no. 2, p. 026039, 2019.
[53] L. N. Awad, A. Esquenazi, G. E. Francisco, K. J. Nolan, and A. Jayaraman, "The rewalk restore^{TM} soft robotic exosuit: a multi-site clinical trial of the safety, reliability, and feasibility of exosuit-augmented post-stroke gait rehabilitation," *Journal of neuroengineering and rehabilitation*, vol. 17, no. 1, pp. 1–11, 2020.
[54] G. Durandau, D. Farina, G. Asín-Prieto, I. Dimbwadyo-Terrer, S. Lerma-Lara, J. L. Pons, J. C. Moreno, and M. Sartori, "Voluntary control of wearable robotic exoskeletons by patients with paresis via neuromechanical modeling," *Journal of neuroengineering and rehabilitation*, vol. 16, no. 1, p. 91, 2019.
[55] F. L. Haufe, P. Wolf, J. E. Duarte, R. Riener, and M. Xiloyannis, "Increasing exercise intensity during outside walking training with a wearable robot," in *2020 8th IEEE RAS/EMBS International Conference for Biomedical Robotics and Biomechatronics (BioRob)*. IEEE, 2020, pp. 390–395.
[56] S. Kim, M. A. Nussbaum, M. I. M. Esfahani, M. M. Alemi, S. Alabdulkarim, and E. Rashedi, "Assessing the influence of a passive, upper extremity exoskeletal vest for tasks requiring arm elevation: Part i–"expected" effects on discomfort, shoulder muscle activity, and work task performance," *Applied ergonomics*, vol. 70, pp. 315–322, 2018.

Nicola Lotti is a Postdoc Researcher at Heidelberg University (Germany) at the Institute of Computer Engineering (ZITI), under the supervision of Professor Lorenzo Masia. He received his bachelor's degree in biomedical engineering (July 2014) from University of Bologna and his master's degree in Bioengineering (curriculum Neuroengineering and bio-ICT) from the University of Genoa (October 2016). In November 2016 he started his PhD in Bioengineering and Bioelectronics at the University of Genoa working at the Department of Informatics, Bioengineering, Robotics, and System Engineering under the supervision of Professor Vittorio Sanguneti. His main research interests are in rehabilitation robotics, exoskeleton, and computational models.

Michele Xiloyannis graduated with a Bachelor degree in Biomedical Engineering from the University of Pisa, Italy, in 2013 and obtained a Master of Science in Neurotechnology from the Department of Bioengineering and Computer Science at Imperial College London, in 2014. In early 2015, Michele received the Singapore International Graduate Award (SINGA) Scholarship to join the Robotics Research Center at Nanyang Technological University, working under the supervision of Prof. Lorenzo Masia. He is now a PostDoc in the SMS Lab, working on the development and validation of soft, lightweight wearable robots to support people with mobility disorders in their daily lives.

Francesco Missiroli is a PhD candidate at Heidelberg University (Germany) at the Institute of Computer Engineering (ZITI), under the supervision of Professor Lorenzo Masia. He received his bachelor's degree in Biomedical engineering (September 2016) and his master's degree in Bioengineering from the University of Padua (February 2019). In September 2019 he started his PhD in Computer Science with focus on wearable robotics. His main research interests are in mechanical design, rehabilitation robotics, exoskeletons, and human-machine interfaces.

Casimir Bokranz is a PhD candidate at the Institute of Computer Engineering (ZITI) under the supervision of Professor Lorenzo Masia, located at Heidelberg University (Germany). He started his studies at university of applied science Ulm (Germany) and received his bachelor's degree in Mechatronics in March 2019. In June 2021 he graduated at Heidelberg University in Computer Engineering with specialisation in "Robotics, Haptics and Biomechanics". His main research interests are human machine interface and wearable assistive technologies.

Domenico Chiaradia is a PostDoc in the Human-Robot Interaction (HRI) area at the Institute of Intelligent Mechanics of the Scuola Superiore Sant'Anna (SSSA), Pisa, Italy. He received the PhD in Robotics from the SSSA, in 2018. He received the B.S. and M.S. degrees in control theory and automation engineering from the Polytechnic University of Bari, Italy, in 2011 and 2014 respectively. His research is focused on the design and control of exoskeletons and exosuits for assistance, force and torque control, control of haptic interfaces and physical human-robot interaction strategies.

Antonio Frisoli is Full Professor of Engineering Mechanics and Robotics at Scuola Superiore Sant'Anna (SSSA), where he leads the Human-Robot Interaction (HRI) area at the Institute of Intelligent Mechanics. He received his PhD (2002) in Industrial and Information Engineering from SSSA, Italy and the MSc (1998) in Mechanical Engineering, minor Robotics, from University of Pisa, Italy and in Industrial Engineering from SSSA (1998). He is IEEE senior member, associate editor for IEEE Robotics Automation Magazine and covers several scientific and editorial roles in scientific societies (Eurohaptics, ICORR), international conferences and journals. His research interest are in the area of collaborative robotics, rehabilitation robotics, wearable robotics and exoskeletons, multimodal interaction and haptics, wearable devices and virtual reality.

Robert Riener is Full Professor for Sensory-Motor Systems at the Department of Health Sciences and Technology, ETH Zurich. He has been Assistant Professor for Rehabilitation Engineering at ETH Zurich since May 2003. In June 2006 he was promoted to the rank of an Associate Professor and in June 2010 to the rank of a Full Professor. He studied mechanical engineering at TU München and University of Maryland, USA, from 1988 till 1993. He received the Dipl.-Ing. degree and the Dr. degree from the TU München in 1993 and 1997, respectively. His current research interests involve human motion synthesis, biomechanics, and rehabilitation robotics.

Lorenzo Masia is Full Professor in Medical Technology and Biorobotics at Heidelberg University (Germany) at the Institute of Computer Engineering or Institut für Technische Informatik, leading the ARIES Lab (Assistive Robotics and Interactive Ergonomic Systems). He accomplished his PhD in "Mechanical Measurement for Engineering" at the University of Padua in 2007. He was visiting student at the Mechanical Engineering Dept. of the Massachusetts Institute of Technology (MIT). He was an Assistant Professor at the School of Mechanical & Aerospace Engineering (MAE) at Nanyang Technological University (NTU) of Singapore and Associate Professor in Biodesign at University of Twente (The Netherlands).